Numerical study on hydrogen mixing for different scramjet Engine combustion chamber configurations

Elsayed Abdelhameed
Toyota Technological Institute

Okamoto, Koki
Toyota Technological Institute

Watanabe, Yasumasa
Toyota Technological Institute

https://doi.org/10.5109/7323356

出版情報：Proceedings of International Exchange and Innovation Conference on Engineering & Sciences (IEICES). 10, pp.825-830, 2024-10-17. International Exchange and Innovation Conference on Engineering & Sciences
バージョン：

Numerical study on hydrogen mixing for different scramjet Engine combustion chamber configurations

Elsayed Abdelhameed[1,2], Koki Okamoto[1], Yasumasa Watanabe[1]
[1]Toyota Technological Institute, 468-8511 Nagoya, Japan
[2]Department of Mechanical Engineering, Faculty of Engineering, Kafrelsheikh University, Egypt
Corresponding author email: elsayedtawfeeq@yahoo.com

Abstract: *This study investigates fuel mixing within a scramjet engine combustion chamber using computational fluid dynamics (CFD) simulations. Employing the Reynolds-Averaged Navier-Stokes (RANS) equations, the Shear Stress Transport (SST) turbulence model, and the energy equation, we model hydrogen fuel mixing in the scramjet's cold flow regime. Simulations, conducted using OpenFOAM software and the 'reactingFoam' solver, focus on evaluating the mixing efficiency and total pressure loss across different engine geometries, including cavity, strut-cavity, and double-cavity-strut configurations. Results show that shockwave interactions significantly influence the flow dynamics, with the strut-cavity configuration yielding the highest fuel diffusion and mixing efficiency. The study validates the model against experimental data from the German Aerospace Center (DLR), highlighting the impact of engine design on scramjet performance.*

Keywords: Scramjet engine; Supersonic flow; Hydrogen; strut; cavity.

1. INTRODUCTION

The Scramjet engine is a promising propulsion engine for future hypersonic transportation [1]. Because of these far-reaching potential uses, hypersonic propulsion research has attracted a lot of attention during the last several decades. Scramjets typically use a combination of gas, liquid, or solid fuels as their primary fuel source [2]. The benefits of gaseous and liquid fuels include the ability to precisely control the fuel flow, a high specific impulse, and excellent combustion efficiency. On the other side, there are a few problems that come with them, such as potential hazards when handling, a low volume-specific impulse, and unstable combustion. In contrast, solid rocket fuels have a reputation for being easy to work with, have a straightforward structure, and have very stable combustion. Although solid fuels have many advantages, they also have several drawbacks, such as poor combustion efficiency, fuel adjustment difficulty, and sensitivity to storage aging.

An optimized injection system is crucial for scramjet engines to achieve higher performance [3]. This is because it improves flame stabilization and fuel-air mixing. There are several engineering contexts in which transverse jet injection into supersonic crossflows is utilized. Researchers have explored numerous injection techniques for fuel mixing in supersonic crossflow. While axial injection using streamwise vortices results in better near-field or macro-mixing, the commonly used method of transverse injection results in high total pressure loss [4]. Before this, other methods like ramp, cavity-assisted, pylon-aided, angled injection, and injection through strut were also investigated [5]. Scramjets can benefit from using cavity-based flame holders to improve flame stabilization. Because they don't get in the way, these flame holders reduce aerodynamic heating, drag, and total pressure loss; hence, they've seen widespread use. Incorporating flame holders based on cavities allows scramjet engines to improve combustion stability and efficiency, which helps with the problems caused by different types of fuel and their combustion properties.

Choubey and Pandey [6]simulated the flow field in a double-strut and double-strut + wall injectors scramjet combustor. The simulation was carried out by combining the two-dimensional Reynolds-Averaged Navier-Stokes (RANS) equations, the two equation Shear stress transport k-ω turbulence model, and the finite-rate/eddy-dissipation reaction model. According to the simulation results, strut wall injection methods, which produce a large separation region, are inferior to the strut injection method. Jianwen and Jialing [7] performed a numerical simulation of a single strut using Navier-Stokes equations combining the k-ω two-equation turbulence model and the flamelet model. These simulation results were compared with experimental data and showed good qualitative and quantitative agreement. For this reason, the interaction between turbulence and combustion in a scramjet cannot be ignored. Choubey and Pandey [8] also investigated the effect of attack angle on a double-strut scramjet combustor by using a finite rate chemistry model as a combustion model. In the case of no angle of attack, the vortexes that form around the struts help mix the air and fuel more efficiently, resulting in a more efficient combustion compared to when there is an angle of attack.

The study of fuel mixing for scramjet engines is elevated to a novel stage by this research. To start with, a solid foundation for correctly modeling the combustion chamber's high-speed flow dynamics can established by employing the Reynolds-Averaged Navier-Stokes (RANS) equations in conjunction with the Shear Stress Transport (SST) turbulence model. Secondly, to accurately assess the mixing efficiency and the effects of various geometrical configurations, the study centers on a cold case scenario, which separates the fuel mixing process from combustion effects. Also, a new way to analyze shockwave interactions is to use the reactingFoam solver in OpenFoam to model hydrogen fuel mixing in supersonic flows. Lastly, improved fuel-air mixture quality is greatly affected by engine design, and new performance metrics like fuel diffusion height provide a thorough way to evaluate engine performance. These ground-breaking additions shed light on how to optimize scramjet engines, which in turn opens the door to hypersonic propulsion systems that are more effective and efficient.

2. GEOMETRY MODELING AND COMPUTATIONAL GRID

This research employs computational fluid dynamics (CFD) to simulate the flow and fuel mixing within the scramjet engine combustion chamber. The study uses the Reynolds-Averaged Navier-Stokes (RANS) equations as the primary governing framework. The model calculates only the fuel mixing in the domain not considering the combustion process (i.e., cold case). Hydrogen, the chosen fuel, necessitates the inclusion of the species transport equation, while the Shear Stress Transport (SST) turbulence model is utilized to compute viscosity. The energy equation is coupled in the model due to the critical influence of high-temperature regions resulting from shock interactions. Simulations are conducted using the OpenFOAM software with the 'rectingFoam' compressible solver to model the flow dynamics accurately [9].

Figure 1 shows the experimental setup and numerical setup of the DLR combustor. At Ma = 2, air is introduced into the combustor through a 40 mm wide and 50 mm high entry. After 60 mm from the entry, the top wall begins to diverge at a 3° angle. The flame stabilizer, a 32-mm-long and 6-mm-thick wedge-shaped strut with a 1 mm diameter hole for H_2, was positioned 35 mm downstream of the entry. At a static temperature of 340K and a pressure of 0.11 MPa, the air is accelerated through a Laval nozzle and introduced into the combustor. The air has the following chemical composition: $Y_{O2} = 0.232$, $Y_{H2O} = 0.032$, and $Y_{N2} = 0.736$. Hydrogen is introduced at sonic speed and a temperature of 250 K. The mesh contains a total of 1,306,588 cells with minimum size near the walls and the fuel injector 1e-4 m, and maximum size is 4e-4 m.

The concept of generating the mesh is the same with refinement near the injection and in the fuel path. The number of cells is around 1,500,000 for the cases.

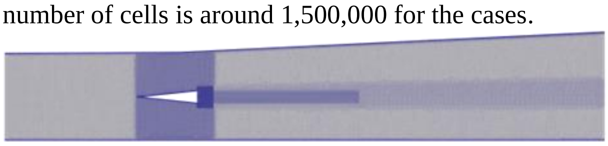

Fig. 1 The applied mesh grid.

3. NUMERICAL METHODOLOGY

The two-dimensional compressible Reynolds-averaged Navier Stokes (RANS) equations coupled with the SST k-ω turbulence model are employed to conduct the following studies, and the SST k-ω turbulence model can be with confidence to investigate the flow field properties induced by the transverse jet.

3.1 Solver details and turbulence model

The governing equations in this study are as follows [10]:

Continuity equation

$$\frac{\partial \rho}{\partial t} + \frac{\partial}{\partial x_i}(\rho u_i) = 0 \qquad 1$$

Momentum equation

$$\frac{\partial}{\partial t}(\rho u_i) + \frac{\partial}{\partial x_i}(\rho u_i u_j) = -\frac{\partial P}{\partial x_i} + \frac{\partial}{\partial x_i}(\tau_{ij}) \qquad 2$$

Energy equation

$$\frac{\partial}{\partial t}(\rho e_t) + \frac{\partial}{\partial x_i}(\rho h_t u_j) = \frac{\partial}{\partial x_i}(\tau_{ij} u_i - q_i) \qquad 3$$

SST $k-\omega$ model

$$\frac{\partial}{\partial t}(\rho k) + \frac{\partial}{\partial x_i}(\rho k u_i) = \frac{\partial}{\partial x_j}\left(\Gamma_k \frac{\partial k}{\partial x_j}\right) + \tilde{G}_k - Y_k + S_k \qquad 4$$

$$\frac{\partial}{\partial t}(\rho \omega) + \frac{\partial}{\partial x_i}(\rho \omega u_i) = \frac{\partial}{\partial x_j}\left(\Gamma_\omega \frac{\partial \omega}{\partial x_j}\right) + \tilde{G}_\omega - Y_\omega + D_\omega + S_\omega \qquad 5$$

In these equations $\tilde{G}_k$ and G_ω represents the generation of turbulent kinetic energy due to mean velocity gradients and generation of $\omega. \Gamma_k$ and Γ_ω represent the effective diffusivity of k and ω respectively. Y_k and Y_ω represents the dissipation of k and ω due to turbulence. D_ω , is defined as the cross-diffusion term and it is written as follows,

$$D_\omega = 2(1 - F_t)\rho\sigma_{\omega,2}\frac{1}{\omega}\frac{\partial k}{\partial x_j}\frac{\partial \omega}{\partial x_j} \qquad 6$$

where the blending function F_t is defined as

$$F_t = \tanh\left(\arg_1^4\right) \qquad 7$$

Where

$$\arg_1^4 = \min\left[\max\left(\frac{\sqrt{k}}{C_\mu \omega y^1}, \frac{500\vartheta}{y^2\omega}\right), \frac{4\rho\sigma_{\omega,2}k}{CD_{k\omega}y^2}\right] \qquad 8$$

Here y is defined as the normal distance to the wall and $CD_{k\omega}$ is the positive portion of the cross-diffusion term.

3.2 Engine performance

Scramjet engine performance is evaluated using combustion efficiency, mixing efficiency, and total pressure loss [11]. In this study, a cold case is being studied and the performance of the engine is being evaluated based on the mixing efficiency and total pressure at a different engine cross-section. The mixing efficiency can be calculated based on the following equation [12].

$$\eta_{\text{mix}}(x) = \frac{\int \alpha\rho Y_{H_2} u dA}{\dot{m}_{H_2}(x)} \qquad 9$$

$$\alpha = \begin{Bmatrix} \frac{1}{\varphi}; \varphi \geq 1 \\ 1; \varphi < 1 \end{Bmatrix} \qquad 10$$

Here $\alpha =$ function of equivalence ratio; $\dot{m}_{H_2}(x) =$ total H_2 mass flux at location x .
Total pressure at each location x can be computed using the following formula [13].

$$p_o(x) = \frac{\int p_o \rho u dy}{\int \rho u dy} \qquad 11$$

While the mixing equation describes how much fuel is being mixed within the stoichiometric limit describing the quality of the fuel mixing, this equation does not calculate the total mixed fuel area or quantify the area covered by the fuel. In this study, we propose considering the fuel diffusion height along the engine as a parameter to calculate the engine performance as the aim of proposing different geometries or injection methods is to get as much mixed air with fuel as possible. The diffusion fuel height is calculated based on the following equation.

$$\text{Fuel\_diffusion\_height} = \begin{cases} \dfrac{\int_a^b dy_{H2}}{\int_a^b dy} & \text{if } \int_a^b dy \neq 0 \\ 0 & \text{if } \int_a^b dy = 0 \end{cases} \qquad 12$$

$$dy_{H2}(y) = \begin{cases} dy & \text{if } 0.003 < F/A < 0.214 \\ 0 & \text{else} \end{cases} \qquad 13$$

$$F/A = {Y_{H_2}}\big/{1 - Y_{H_2}} \qquad 14$$

4. VALIDATION

In this study, we used the German Aerospace Center (DLR) engine to validate the constructed model [6]. Fig. 2 illustrates the simulation results for wall pressure versus the experimental results and the literature. The simulation results show an agreement with the experimental results. In this study a grid mesh convergence study was done to ensure the mesh quality and the difference in the wall pressure was noticed to change by less than 0.5% between the coarse and fine mesh.

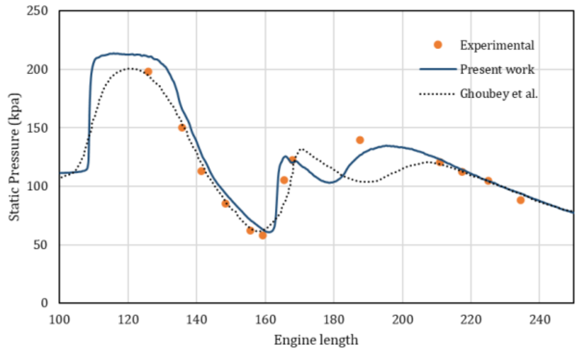

Fig. 2 Wall static pressure DLR, and Goubey et al.[10].

5. RESULTS AND DISCUSSIONS

The simulated engine has two inclined walls with 1° from horizontal and the strut has a wedge angle reaching 12°. the dimensions are explained in the Fig. 3. The red arrow in the figure illustrates the injection port for each design. Generally, the outer dimensions and the strut length are constant across the cases.

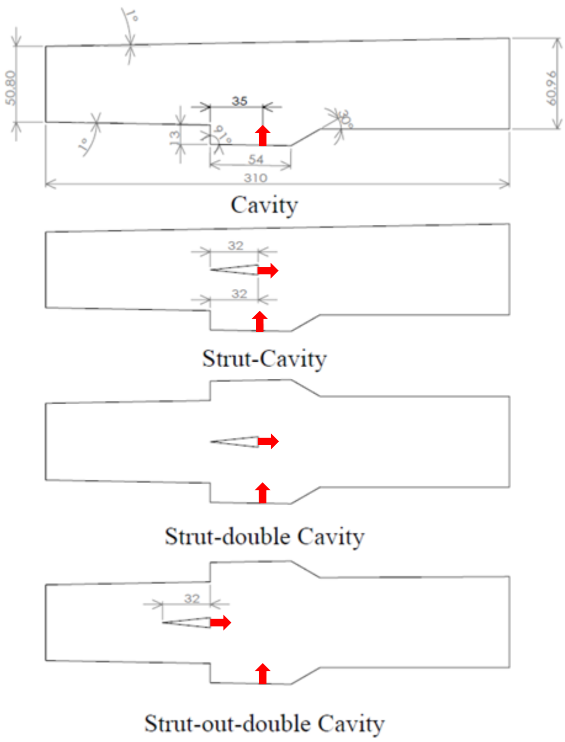

Fig. 3 Scramjet engine specifications. The main geometric dimensions are the same and the double cavities are symmetrical about the centerline.

The following sections, a detailed analysis and discussion of the proposed different arrangements of strut and cavity in the scramjet engine. As the supersonic flow passes through the engine vicinity, shock waves are formed due to the flow interaction with the geometry of the engine. The cavity case is the base case in this study in which 2 shock waves are formed from the hydrogen injection from the cavity floor and from the step at the end of the cavity as shown in Fig. 4. Meanwhile, the shockwaves and their reflections became more intense and complex when including the strut with the cavity. In the case of strut-cavity, the reflected shock wave from the strut body interacts with the boundary layer and leads to a standing shock wave with a slight curvature at 82kPa. When comparing this standing shock wave with the double-cavity-strut design, the increase in the cross-section area by utilizing a double cavity leads to mild reflected shock waves.

Both velocity and temperature have a strong dependency on the shock waves and their reflections. From Fig. 5, the temperature of the stream increases in the areas where the shock waves reflect or interact with another reflected shock wave. Around the tip of the cavity step in the cavity case, a slight increase in the stream temperature can be noticed. This change in the stream temperature is intensive in the strut-cavity case where the reflected shock wave interacts with the engine wall boundary layer on the upstream side of the strut and at the downstream section where the reflected shockwave from the step interacts with the reflected wave from the wall just in the middle of the stream and in front of the injected hydrogen from the strut. In the other two cases with double-cavity-strut, the temperature increase varies depending on the shock wave reflection interaction. For example, moving the strut upstream to be outside of the double cavity, leads to intense reflected waves from the cavity step and as a result an increase in the local stream temperature.

Fig. 6 illustrates the mass fraction of the hydrogen in the domain. Even though hydrogen is an extreme molecule that can penetrate the ambient when being injected, the hydrogen injection and mixing into the supersonic flow is not straightforward as the time available for mixing is critically limited due to the very high fluid speeds, in this figure, an overall of the hydrogen can shed the light on the importance of the engine geometry on the hydrogen-air mixture. In the cavity geometry, the fuel is being recirculated into the cavity that works as a flame holder, and obviously, the hydrogen fuel cannot penetrate the mainstream. Adding the strut to the cavity generates a hydrogen stream in the middle of the flow stream. Meanwhile, a close look at the flow domain shows the effect of the reflected shock waves on the hydrogen stream in two points; first, in the area near the strut tip where the standing shock wave is formed, the hydrogen fuel traveled upstream as the shockwave leads to decrease the flow speed. Second, the area downstream where the reflected shock wave from the cavity interacts with the hydrogen stream leading to a shift in the stream and as a result covering a wider area in the flow domain. In the strut with the double cavity, the reflection of the shockwave from the strut body to the step wall eliminates the hydrogen to move directly downstream but recirculates in a narrow area just in front of the injection port in the cavity, and the majority of the upstream of the cavity.

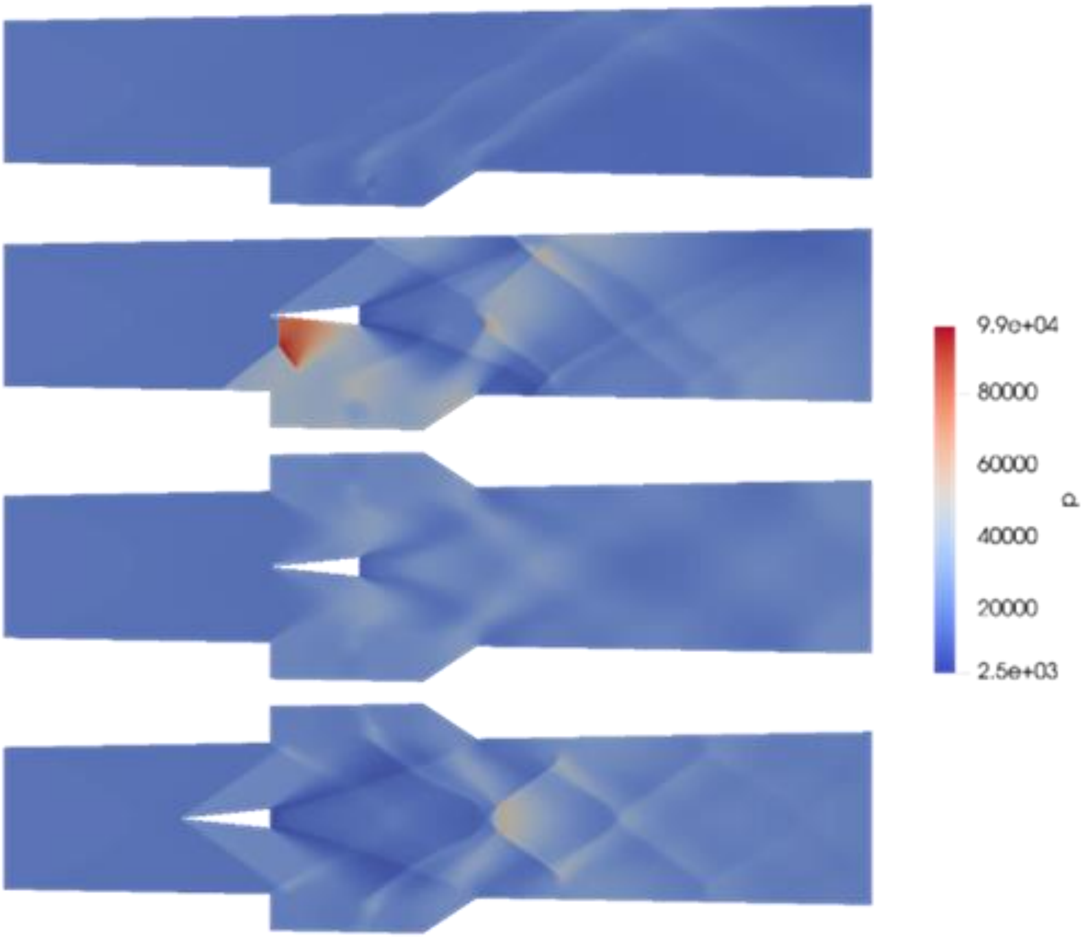

Fig. 4 Numerically simulated pressure contour for different test cases

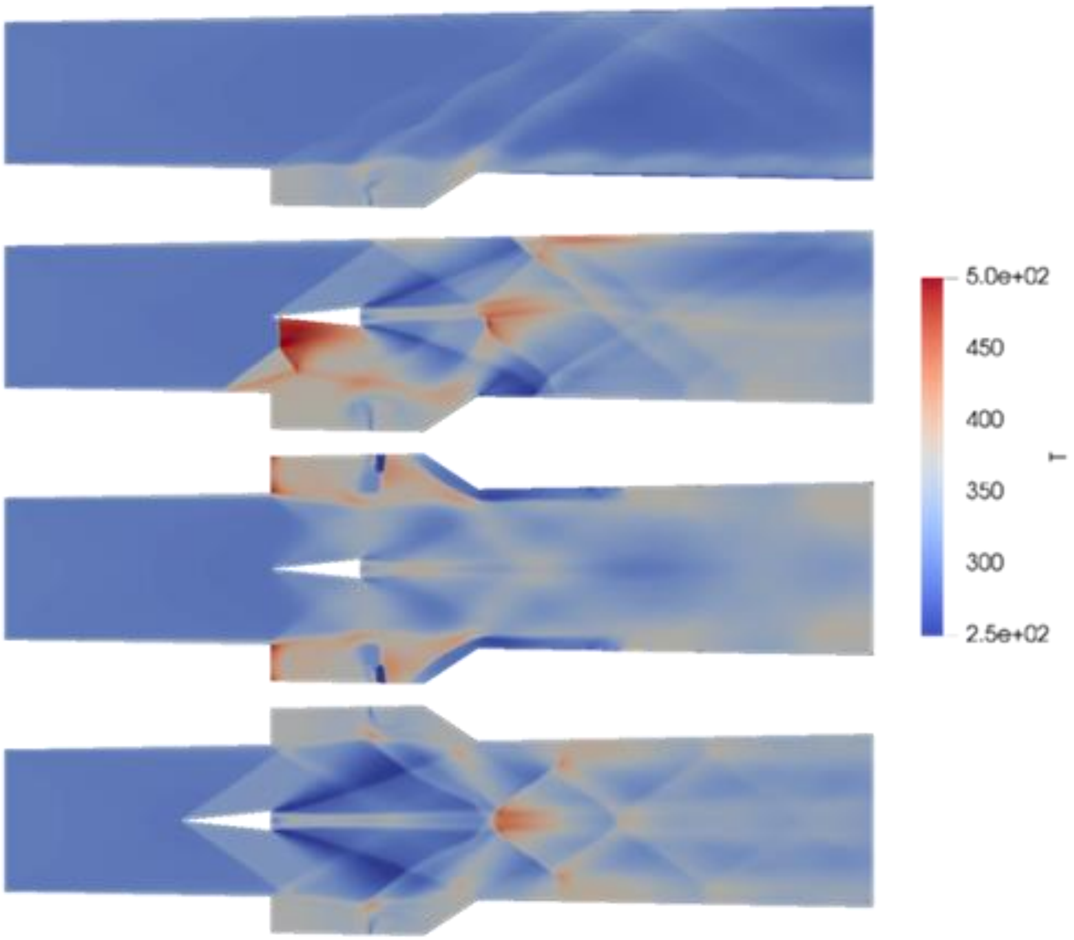

Fig. 5 Numerically simulated Temperature contour for different test cases

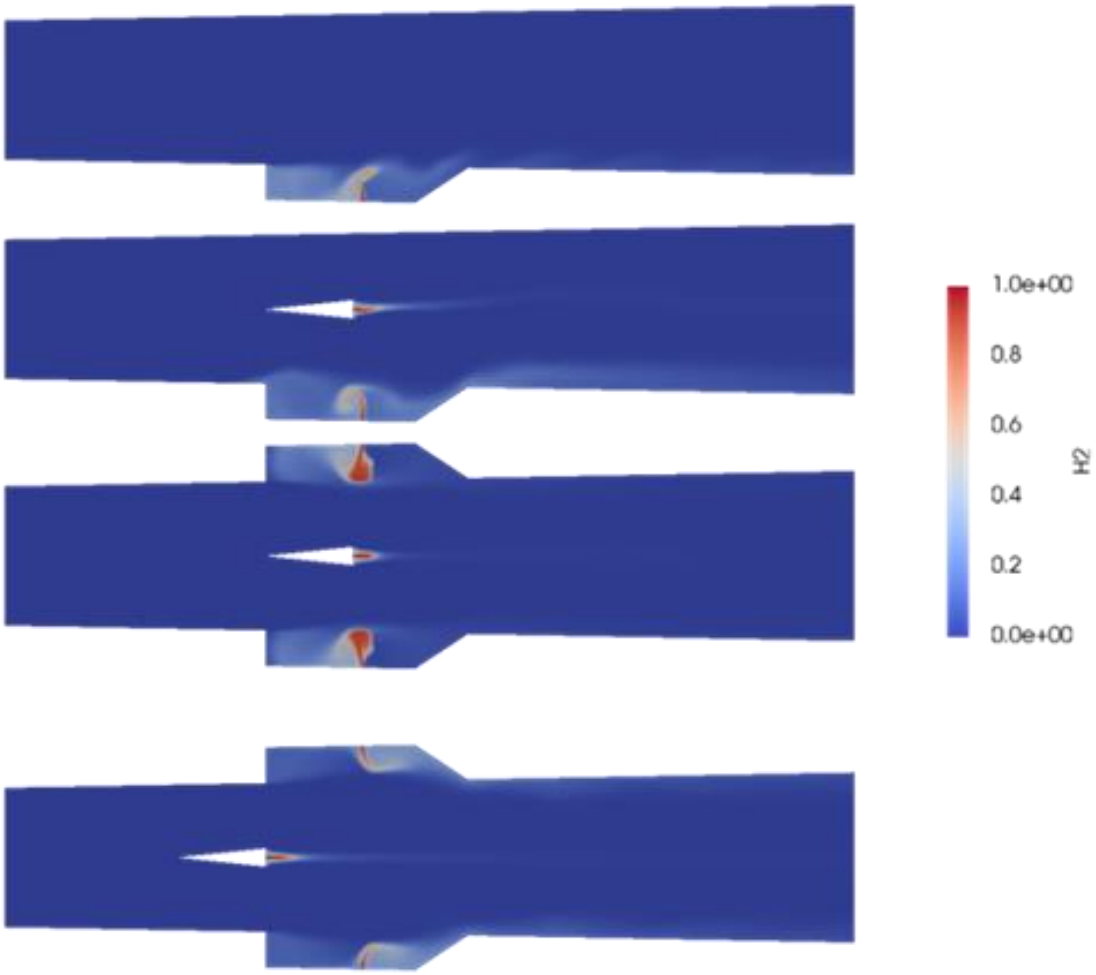

Fig. 6 Numerically simulated Hydrogen mass fraction contour for different test cases

To quantify the performance of the scramjet engine in each geometry, weighted average calculations were done for the hydrogen and the total pressure across the engine length. A Python code was established to calculate the total pressure at each cross-section. Fig. 7 shows the normalized total pressure for the different test geometries. Due to using the strut in the flow path, the total pressure loss increases along the engine length due to the increase in the shock waves and its reflection that leading to increase the energy loss in the flow path. The decrease in the total pressure in the first section is linear and almost identical in all cases except for the strut-out-double cavity where the total pressure decreases in the location of the strut. The effect of standing shock wave in the case of strut-cavity is obvious with its step reduction of around 0.8 m of engine length. Meanwhile, the total pressure reduction in the case of strut-double-cavity shows the maximum reduction among the four cases.

Among all known fuels, hydrogen has the highest flammability range. Hydrogen with a mixing percentage of 4-75 % with air can theoretically sustain combustion these percentages are almost equal ($0.003<\boldsymbol{F/A}>0.214$). In the present work, the mixing efficiency and the fuel diffusion ratio at each engine length have been calculated. The mixing efficiency for the different geometries exceeded 85% around 0.16 m from the engine length. The strut_out_double_cavity shows the maximum mixing efficiency that can be attributed to the extra divergent area just downstream to the strut, whilst, the other two cases show a lower mixing efficiency compared to the cavity case. One more parameter has been considered to evaluate the fuel mixing in the stream which is the fuel diffusion ratio. Strut-cavity case shows the maximum enhancement in the fuel diffusion reaching 0.366 from the total engine height compared to 0.141 from the total engine height at the outlet for the cavity case. The enhancements in the fuel mixing diffusion reached 160%, 64%, and 84% for the strut-cavity, strut-out-double-cavity, and strut-double-cavity, respectively.

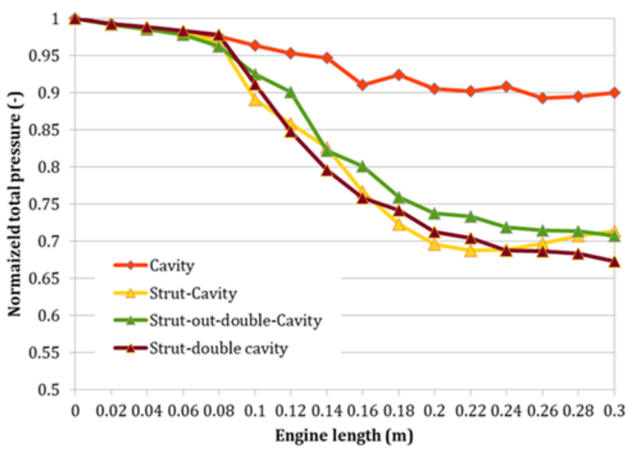

Fig. 7 Normalized total pressure over the engine length.

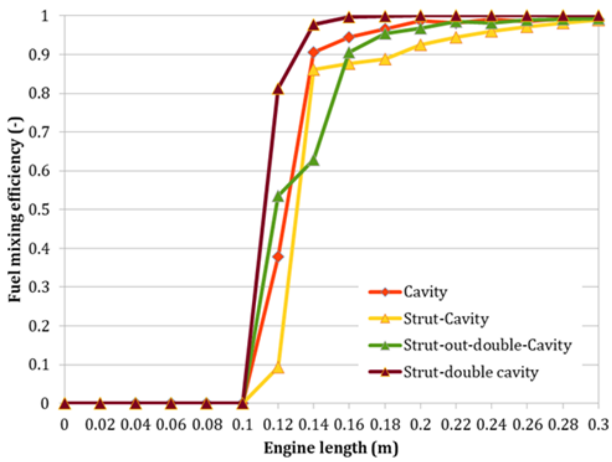

Fig. 8 Mixing efficiency over the engine length.

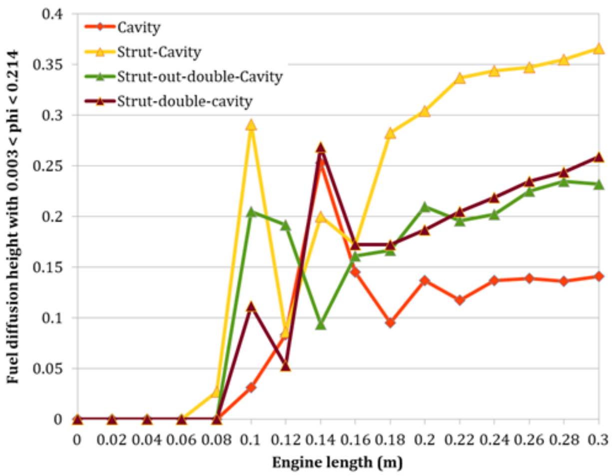

Fig. 9 Fuel diffusion height for the mixed fuel within the flammability range.

6. Conclusions

The CFD simulations of the scramjet engine combustion chamber reveal that engine geometry plays a crucial role in fuel mixing and flow dynamics. The inclusion of struts and cavities introduces complex shockwave interactions that affect hydrogen diffusion and overall engine performance. Among the tested configurations, the strut-cavity design demonstrated the most significant enhancement in fuel mixing, achieving a 160% improvement in fuel diffusion compared to the cavity-only configuration. The strut-out-double-cavity configuration exhibited the highest mixing efficiency at 85% along the engine length. These findings underscore the importance of optimizing engine geometry to maximize fuel-air mixing efficiency and minimize total pressure loss, thus improving scramjet engine performance. Future work should explore the combustion process and further refine the geometrical configurations to achieve optimal scramjet operation.

7. ACKNOWLEDGEMENT

This research was partially under support of JSPS grant no. 23K26305.

8. REFERENCES

[1] Zhou W, Xing K, Dou S, Yang Q, Xu X. Distribution characteristics of a supercritical hydrocarbon fuel jet injected into a high-speed crossflow. Fuel 2023;333. https://doi.org/10.1016/j.fuel.2022.126497.

[2] Elliott S, Lax P, Leonov SB, Carter C, Ombrello T. Acetone PLIF visualization of the fuel distribution at plasma-enhanced supersonic combustion. Exp Therm Fluid Sci 2022;136. https://doi.org/10.1016/j.expthermflusci.2022.110668.

[3] Ding H, Zhuo C, Deng H, Hu W, Chen X. Numerical study on coupled flow characteristics of a gas-solid two-phase jet in a supersonic crossflow. Int J Multiph Flow 2023;168. https://doi.org/10.1016/j.ijmultiphaseflow.2023.104583.

[4] Sekar A, Vaidyanathan A. Mixing enhancement of ethylene secondary jet injected into supersonic cross-flow using curved pylon. Acta Astronaut 2023;210:253–67. https://doi.org/10.1016/j.actaastro.2023.04.046.

[5] Li Z, Abu-Hamdeh NH, Bantan RAR, Musa A. Effects of downstream ramp on the fuel diffusion of single cross jet at supersonic flow: Computational study. Int J Heat Mass Transf 2022;195. https://doi.org/10.1016/j.ijheatmasstransfer.2022.123183.

[6] Choubey G, Pandey KM. Effect of different strut + wall injection techniques on the performance of two-strut scramjet combustor. Int J Hydrogen Energy 2017;42:13259–75. https://doi.org/10.1016/j.ijhydene.2017.04.024.

[7] Xing JW, Le JL. Application of flamelet model for the numerical simulation of scramjet. Shiyan Liuti Lixue/Journal Exp Fluid Mech 2008;22:40–5.

[8] Choubey G, Pandey KM. Effect of variation of angle of attack on the performance of two-strut scramjet combustor. Int J Hydrogen Energy 2016;41:11455–70. https://doi.org/10.1016/j.ijhydene.2016.04.048.

[9] Shen Z, Yu S, Zheng S, Nofal TA, Musa A, Li Z. Numerical study of multi-jet with upstream divergent ramp at supersonic cross flow. Aerosp Sci Technol 2022;127. https://doi.org/10.1016/j.ast.2022.107689.

[10] Choubey G, Solanki M, Patel O, Devarajan Y, Huang W. Effect of different strut design on the mixing performance of H2 fueled two-strut based scramjet combustor. Fuel 2023;351:128972. https://doi.org/10.1016/j.fuel.2023.128972.

[11] Huang W, Wu H, Du Z bo, Yan L, Choubey G. Design exploration on the mixing augmentation induced by the oblique shock wave and a novel step in a supersonic flow. Acta Astronaut 2021;180:622–9. https://doi.org/10.1016/j.actaastro.2020.12.058.

[12] Jian D, Chao H, Qiuru Z, Fei X. A numerical study on flow structure and combustion mechanism of supersonic mixed inflow with transverse jet. Aerosp Sci Technol 2021;116. https://doi.org/10.1016/j.ast.2021.106865.

[13] Feng Y, Luo S, Song J, Xia K, Xu D. Numerical investigation on the combustion characteristics of aluminum powder fuel in a supersonic cavity-based combustor. Appl Therm Eng 2023;221. https://doi.org/10.1016/j.applthermaleng.2022.119842.